



Thermophysical and Mechanical Properties of Clay-Based Composites Developed with Hydrothermally Calcined Waste Paper Ash Nanomaterial for Building Purposes

Ubong Williams Robert¹ · Sunday Edet Etuk² · Joseph Bassey Emah¹ · Okechukwu Ebuka Agbasi³  · Ubong Asuquo Iboh¹

Received: 28 November 2021 / Accepted: 15 February 2022 / Published online: 14 March 2022
© The Author(s), under exclusive licence to Springer Science+Business Media, LLC, part of Springer Nature 2022

Abstract

Just like disposal of waste papers by indiscriminate dumping, stabilisation of clay soil using cement or by firing has a potential adverse effect on the environment and public health. Thus, the essence of this work was to investigate the feasibility of chemically modifying clay soils using waste papers in order to solve the disposal problems and also develop clay-based composites suitable for building purposes. Hydrothermally calcined waste paper ash nanomaterial (HCWPAN) was prepared from assorted waste papers and used to separately develop composites with white clay matrix (WCC) and yellow clay matrix (YCC) each at 0 %, 10 %, 20 %, 30 %, and 40 % volumetric proportions of replacement. Three representative samples were developed in each case. Apparent porosity, water absorption, bulk density, sorptivity, thermal conductivity, specific heat capacity, volumetric heat capacity, thermal diffusivity, thermal lag, flaking concentration, flexural strength, and compressive strength were investigated for all the samples. For satisfactory performance during service, the optimum content level of the HCWPAN was found to be 10 % in the samples. Though the WCC sample possessed greater compressive strength (4.029 ± 0.002) MPa than the value (2.895 ± 0.002) MPa obtained for the YCC sample at that level, the latter exhibited greater potential for enhancement of thermal comfort as a walling element in buildings. Also, reductions from 8.98 % to 8.00 % and 13.30 % to 12.575 % were observed in water absorption of the resulting WCC and YCC samples, respectively. From the technical–economic viewpoint, the HCWPAN is a promising material for clay soil modification for building purposes.

Keywords Angle of repose · Building materials · Flexural strength · Sorptivity · Thermal conductivity · Thermal lag

✉ Okechukwu Ebuka Agbasi
agbasi.okechukwu@gmail.com

Extended author information available on the last page of the article

1 Introduction

In recent years, the technological revolution of this twenty-first century has brought about pronounced impacts in many spheres of human life through utilisation of natural resources. For instance, papers are manufactured from cellulose pulp of wood [1] and used daily for a number of different applications among which are printing (books and newspapers), packaging (carton), writing, drawing, industrial and construction purposes, and so on. In year 2017 World Facts report, it was indicated that out of 215 125 083 tons of paper produced by 10 countries globally, China took the lead followed by the United States and then Japan with production capacity of 99 300 000 tons, 75 083 000 tons and 26 627 000 tons respectively [2]. Equally, O'mara [3] observed that 300 million tons of papers are produced yearly all over the world. Based on the fact that paper has diverse applications (depending on its dry weight which, usually, is between 70 and 300 gsm inclusive), and it remains one of the necessities of civilisation, it is obvious that there can be no halt in its production.

As it is applicable to other solid materials, papers and paper products that are no longer valuable are usually treated as solid wastes and the quantity of papers considered as waste materials increases on daily basis. Adeniran *et al.* [4] estimated 4.83 tons to be an average waste paper generation per day. Also, Arazo [5] found, as of 2015, that waste paper and paper products constituted a total of 82.82 % of the overall weight of wastes generated from four streams in the campus of Misamis Oriental State College of Agriculture and Technology (MOSCAT) located in the southern part of Philippines. The composition of solid wastes generated changes with time and varies from municipality to municipality [6] with paper and paper products constituting approximately 25 % to 40 % on global scale [7]. In Nigeria and other developing countries, solid wastes management is very ineffective nowadays because funding, legislation/implementation of policy, recovery and recycling programmes are poorly handled. Consequently, the prevalent disposal methods for waste papers and related products are by indiscriminate dumping and open burning. These practices are detrimental to the environment and public health since the dumpsites can become avenues for spread of diseases and burning of waste papers in the open can lead to increase in the amount of carbon dioxide in the atmosphere.

Soil is another available natural resource that is of great importance to humans. The dependence of human beings on natural resources which constitute their environment [8] is clearly manifested in the cases of food and shelter being paramount in the traditional list of immediate basic needs of humans [9]. From agriculture perspective, loamy and sandy soils play very crucial roles in the satisfaction of human needs for food on either subsistence or commercial basis through planting and farming. Observably, clay soil is rather utilised in the form of plasters, bricks or mortars as a traditional construction material for shelter. Since the clay soil exhibits low strength, high level of volumetric change, and susceptibility to water damage, this usage is accompanied with many challenges. Of course, studies have shown that either chemical treatment using Portland cement or thermal

treatment can be adopted to improve the physico-mechanical properties of clay bricks [10–13]. However, thermal treatment usually involves high-energy usage followed by emission of carbon dioxide which is a greenhouse gas and is capable of causing very serious environmental problems. Also, incessant rise in the cost of building/construction materials [14] affects the use of cement as a hydraulic binder for stabilisation purpose, thereby hindering the development. Aside that, production of Portland cement leads to the release of significant amount of carbon dioxide [15] and according to the measured data from European cement kiln emissions, cement industry contributes substantially to environmental pollution with emission of 1.5456 million tons of carbon dioxide yearly [16].

It has been reported that modification of clay soils using fly ash [17], textile ash waste [18], nano silica or nano aluminium oxide and certain other nanomaterials [19, 20] can effectively improve the properties of bricks developed from them for building purposes. Also, researches have revealed that desirable properties of composite ceiling [21] or concrete [22] can be achieved with the use of waste paper ash. This, no doubt, portrays a safe way to manage waste papers. In view of the aforementioned circumstances, this work is designed to investigate the feasibility of utilising waste papers to chemically modify clay soils in order to solve the disposal problems and also develop clay-based composites suitable for building purposes. Specifically, thermophysical and mechanical properties of samples developed using hydrothermally calcined waste paper ash nanomaterial (HCWPAN) with two clay soils of distinct colours will be compared in order to determine their suitability for use as potential walling materials for passively cooled building design. It is hoped that, in addition to enhancing inexpensive and safe building construction, such attempts will consequently become an advantage for brick producers.

2 Experimental Program

2.1 Materials Acquisition and Description

Waste papers, clay soils and water (from bore-hole) were the main materials used to develop test samples in this work. The waste papers were of different types (such as writing papers, newspapers and copier papers) and were sourced from schools, newspaper vendors, and business units/offices. Also, the clay soils were in wet form and plastic in nature but of two distinct colours namely, white and yellow. These materials were sourced in large quantities within Uyo metropolis, Akwa Ibom State, Nigeria.

2.2 Preparation of the HCWPAN

After surface-cleaning of the waste papers, they were shredded into smaller pieces by means of scissors and the pieces obtained were burnt to ash in an incinerator (Model i8-20S) at 850 °C for 1 h. This type of incinerator was used because it has a secondary chamber which allows it to operate without smoke, odours or harmful

emissions. The ash produced was screened (using US mesh No. 60) to remove any accompanying impurity. In order to ensure formation of hydraulically active mineral phases, the sieved ash was hydrothermally calcined by adopting two stages of heat treatment. The first stage involved heating a thorough mixture of the ash and water for 12 h in a Teflon-lined autoclave at 200 °C [23]. In the second stage, the pre-heated precursor was calcined at 750 °C for 4 h in an electric furnace. When it cooled to 35 °C, the as-prepared calcined ash was pulverised using Agate mortar and pestle before it was ball-milled by means of a high-energy ball miller (E_{\max} , manufactured by RETSCH GmbH) at 500 rpm for 6 h. This machine can effectively reduce a material feed from about 5 mm particle size to as fine as less than 80 nm. The hydrothermally calcined waste paper ash nanomaterial prepared was denoted as HCWPAN.

2.3 Analysis of the Clay Soils and HCWPAN

The clay soils were first made to become moisture-free by sun-drying them for several days and also weighing daily at intervals of 2 h until a constant mass was obtained for more than ten consecutive measurements in each case. After that, they were crushed separately by means of hammer and the quantity of each of them that passed US mesh No 10 was utilised in this study. Then, the HCWPAN and sieved clay soils were each divided into two portions. By employing fixed funnel method [24] with some modifications, the static angle of repose was determined using one portion, each, of the materials. A plastic funnel was fixed and a particular material was poured from the funnel at a certain height onto a selected base with known roughness properties. While the conical shape of the material heap was forming, the height (between 2.0 cm and 6.5 cm inclusive) and radius (half of diameter) of the heap were measured until five pairs of such parameters were obtained. The plot of height against radius permitted the determination of static angle of repose, \emptyset based on inverse tangent rule, thus

$$\emptyset = \tan^{-1} (S) \quad (1)$$

where S =slope of the graph.

Also, particle size analysis of the clay soils was carried out by hydrometer method of sedimentation according to the standard procedure stated in [25] and their plasticity index was obtained based on the standard approach captured in [26]. Again, with the aid of X-ray fluorescence analyser (Spectro X-lab 2000), the chemical composition as well as loss on ignition of the HCWPAN and clay soils was determined as per the techniques used by [27, 28].

2.4 Test Samples Fabrication

The remaining portions of the clay soils and HCWPAN were used to develop the test samples. Similar various volume fractions of the HCWPAN were thoroughly mixed with each clay soil material (as shown in Table 1). When consistency was observed, each mixture was moistened with a reasonable quantity of water after which it was

Table 1 Design of the sample formulations

Volume fraction of processed clay soil (%)	100	90	80	70	60
Volume fraction of the HCWPAN (%)	0	10	20	30	40

compacted to have parallel surfaces using a 100 kg load for 24 h. Samples meant for mechanical characterisation were formed in a mould of dimensions 210 mm × 36 mm × 12 mm. Others were developed in a 260 mm × 260 mm × 30 mm mould before they were cut carefully (after drying) into sizes needed for assessment of thermophysical properties. The samples were fabricated in triplicates per formulation and all of them were subjected to continuous sun-drying and weighing until no further reduction in their masses was observed.

2.5 Characterisation

2.5.1 Porosity, Water Absorption and Bulk Density

The apparent porosity and water absorption of each sample were determined in accordance with the standard procedure stipulated in [29]. Immersion was allowed to last for 12 h after the dry weight, W_d had been measured. The suspended weight, W_s and saturated weight, W_a were then obtained and the apparent porosity, φ was calculated as

$$\varphi = \left(\frac{W_a - W_d}{W_a - W_s} \right) 100\% \quad (2)$$

while water absorption, WA was computed as

$$WA = \left(\frac{W_a - W_d}{W_d} \right) 100\% \quad (3)$$

For bulk density determination, the mass of each sample piece was measured using a digital balance (S. METTLER – 600 g) and its bulk volume was obtained by modified water displacement method [30]. In this case, surface-coating of the sample was performed by dipping in a melted waste candle wax (of density $0.914 \text{ g}\cdot\text{cm}^{-3}$). A 100 cm^3 graduated glass cylinder (of external diameter 29.86 mm and thickness 1.56 mm) was also used. The required bulk density was then found as [31, 32]

$$\rho = \frac{M}{V} \quad (4)$$

where ρ = bulk density, M = mass of the sample and V = bulk volume of the sample.

2.5.2 Sorptivity

Sample pieces for sorptivity test were made to be rectangular in shape before some parallel lines were drawn from one end on one side of each of them. The lines were equally spaced (3 mm) and their distances from the end of a sample piece were

noted and considered as the infiltration depths of water. By means of a strong inextensible string, each sample piece was suspended at its other end. A small glass vessel containing foam saturated with cold water at 28 °C was placed directly under the suspended sample. While adjusting the position of the sample, care was taken to ensure that immediately its lower end rested on the foam (Fig. 1), a digital stopwatch (Model TA 228) was turned on to measure the time spent by the water to infiltrate the sample to each depth. From the plot of water infiltration depth against square root of the infiltration time, the sorptivity of the sample was deduced graphically in line with the relation [33]

$$H = S_p \sqrt{t} \quad (5)$$

where H = cumulative water infiltration depth, t = infiltration time, and S_p = sorptivity of the sample.

2.5.3 Specific Heat Capacity and Volumetric Heat Capacity

Using the method described in [34], the specific heat capacity value of each test sample was determined. A stainless steel container was filled with dry sharp river-bed sand to 18 mm of its depth. The sample under investigation was then embedded in the sand, ensuring that it made no direct contact with the container. As the container was heated by means of an electric hotplate (Lloytron E4102WH), the temperature of its content was monitored. When it was observed that the temperature remained unchanged for about 2 min, the sample was quickly transferred by tongs into water contained in a copper calorimeter before stirring was done using a copper stirrer. To obtain the value of final steady temperature of the mixture, temperature-cooling correction value was added to the observed steady temperature value. With assumption of energy conservation in the process, the total quantity of heat lost by the sample was equated to be the

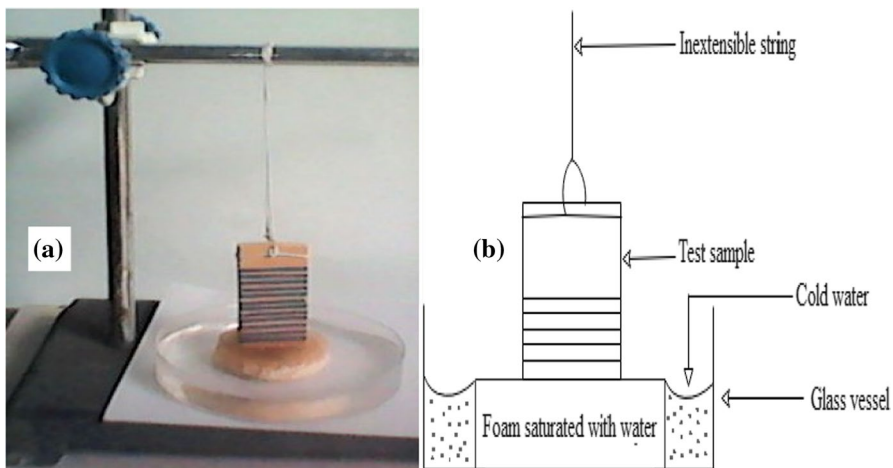


Fig. 1 Set-up diagrams for the sorptivity test (a) experimental, (b) schematic

same as the total quantity of heat gained (by the calorimeter, water, and stirrer). The effective specific heat capacity, c of the sample was then calculated as [35]

$$c = \frac{Q_c + Q_w}{M\Delta\theta} \quad (6)$$

where Q_c = total quantity of heat gained by the calorimeter and stirrer, Q_w = total quantity of heat gained by the water, M = mass of the sample under test, and $\Delta\theta$ = change in temperature of the sample on cooling completely.

The values of bulk density and specific heat capacity obtained for each test sample were then applied to compute the corresponding volumetric heat capacity, C_v , as

$$C_v = \rho c \quad (7)$$

2.5.4 Thermal Conductivity, Thermal Diffusivity, and Thermal Lag

Thermal conductivity test was conducted using Heat Flow Meter (HFM 100 series) in accordance with the standard procedure outlined in [36]. A sample was positioned between two heating—cooling plates and the upper plate powered by stepper motors. One sensor was integrated into each plate to monitor heat flux generated due to the difference in temperature between the top plate and bottom plate at regular intervals. At steady state, the data obtained were used based on Fourier's law for one-dimensional heat flow to determine the effective thermal conductivity value, k thus [37]

$$k = \frac{Qx}{A\Delta T} \quad (8)$$

where x = thickness of the sample, Q = quantity of heat flowing through the sample per second, A = cross-sectional area of the sample, and ΔT = temperature difference between the top and bottom plates of the Heat Flow Meter at steady state.

Also, thermal diffusivity, λ was calculated using the formula [38]

$$\lambda = \frac{k}{C_v} \quad (9)$$

and its value was used to find the thermal lag, T_L on a 24-h basis of external periodic heat flow by applying the equation[35]

$$T_L = \left(\sqrt{\frac{T_p}{4\pi\lambda}} \right) x \quad (10)$$

where T_p = period.

2.5.5 Flaking Concentration

Since the test samples under consideration might undergo wear in the course of their application as building materials, examination of their abrasion resistance was

deemed necessary. This was conducted as flaking concentration test on the samples developed for evaluation of mechanical properties in this work. The initial mass of each test sample was measured after which a very hard shoe brush was used to rub against their two surfaces until 70 strokes of forward and backward movements were made. In order to ensure application of uniform pressure throughout the test schedule, a 0.5 kg weight was attached to the top of the brush. The flaked samples were weighed and decrease in the mass of each of them was determined. By calculation, the flaking concentration, F_c was obtained thus [23]

$$F_c = \left(\frac{\Delta M}{M_i} \right) 100\% \quad (11)$$

where ΔM = decrease in the mass of the sample after being flaked, and M_i = mass of the sample before being flaked.

2.5.6 Flexural Strength and Compressive Strength

In addition, a computerised electromechanical universal testing machine (Model WDW-10) was used to perform flexural strength and compressive strength tests on each sample as stated in [39]. For flexural strength evaluation, three-point bending technique was adopted. This involved suspension of a test sample as a single beam supported at two points and then loading at its mid-point until it fractured. The data obtained were applied in computation of the flexural strength value, σ as described by the relation [21]

$$\sigma = \frac{3FL}{2bx^2} \quad (12)$$

where F = maximum load applied at fracture, L = span length, b = width of the sample under test, and x = thickness of the sample.

As for the compressive strength, the data obtained for the crushing force, P and cross-sectional area, A of each sample were used to compute the value as [40, 41]

$$CS = \frac{P}{A} \quad (13)$$

where CS = compressive strength of the sample.

The tests in this work were carried out at room temperature with ± 2 °C variations. For each test, the three samples developed per percentage composition were used. In each case, the mean of (and standard error in) the values obtained were determined and tabulated. More so, uncertainty in the obtained results of each property was recorded. The values specified for the devices applied in this work to evaluate thermal conductivity, flexural strength, and compressive strength of the samples were adopted. In other cases, the principles documented in NIST Technical Note (1994 edition) were applied and in each case involving derived measurand, propagation calculation was used to determine the required combined standard uncertainty.

Table 2 Particulars of the clay soils and HCWPAN used in the study

Parameters	Materials		
	White clay	Yellow clay	HCWPAN
Form	Dry	Dry	Dry/powdery
Plasticity index, PI	$(27.41 \pm 0.01) \%$	$(19.11 \pm 0.01) \%$	–
Static angle of repose, \emptyset	$(30.01 \pm 0.26)^\circ$	$(28.20 \pm 0.11)^\circ$	$(41.25 \pm 0.47)^\circ$
Particle size	≤ 2.0 mm	≤ 2.0 mm	80.0 nm

The values of PI and \emptyset are obtained from five determinations in each case

Table 3 Chemical parameters of the clay soils and HCWPAN

Major components		Proportion (% wt)		
Name	Formula	White clay	Yellow clay	HCWPAN
Aluminium trioxide (Alumina)	Al_2O_3	40.74	11.63	1.62
Silicon dioxide (Silica)	SiO_2	48.61	57.98	28.02
Ferric oxide	Fe_2O_3	1.34	3.80	1.03
Calcium oxide (Lime)	CaO	0.11	5.68	56.78
Magnesium oxide (Magnesia)	MgO	0.06	3.54	1.29
Potassium oxide	K_2O	1.34	7.79	0.04
Loss on ignition	LOI	4.81	9.13	10.31

3 Results and Discussion

Table 2 shows some basic particulars of the materials utilised to fabricate the test samples. Findings from the chemical composition analysis of each material are presented in Table 3. In Table 4, results of the tests performed on the samples are recorded. The samples that contain 0 % of the HCWPAN are regarded as blank/control/reference samples.

It can be seen in Table 2 that the HCWPAN has the highest value of repose angle, followed by the white clay and then the yellow clay. Based on the fact that angle of repose is inversely proportional to the size of a material's particle [42, 43], it can be adjudged that though particles in the clay soils used in this study are at most 2 mm in size, the white clay contains more particles that are smaller in size compared to the yellow clay whereas the HCWPAN is made up of particles that are the smallest in size. This submission on the clay soils is well supported by the gradation results illustrated in Fig. 2. As revealed, the proportion of the white clay that contains particles ranging in diameter from 0.001 mm to about 0.1 mm is larger than in the case of the yellow clay. By containing nano-sized particles, the HCWPAN can function as filler in a clay matrix in order to form a clay-based composite. Since angles of repose must range from 25° to 30° for excellent flowability and 41° to 45° for passable flow property [44], it implies

Table 4 Results of thermophysical and mechanical tests performed on the developed samples

Particulars	Volume fraction of the HCWPAN in the sample (%)	Values obtained for each property investigated						
		Porosity, ϕ (%)	Water absorption, WA (%)	Bulk density, ρ (kgm^{-3})	Sorptivity, S_p ($10^{-4} ms^{-\frac{1}{2}}$)	Thermal conductivity, k ($Wm^{-1}K^{-1}$)	Specific heat capacity, c ($Jkg^{-1}K^{-1}$)	
Sample code	WCC	0.0	15.38±0.08	8.98±0.07	2329.98±1.07	9.148±0.016	0.3400±0.0004	1575.86±1.87
		10.0	14.69±0.06	8.00±0.03	2298.78±1.48	9.501±0.018	0.2911±0.0004	1593.71±2.16
		20.0	15.91±0.06	9.64±0.05	2006.12±1.26	9.994±0.012	0.2394±0.0002	1741.08±2.66
		30.0	20.01±0.09	11.29±0.05	1878.13±1.38	10.731±0.018	0.2088±0.0004	1842.42±1.75
		40.0	25.39±0.05	14.15±0.07	1772.04±1.12	11.492±0.014	0.1844±0.0003	1947.61±1.76
	YCC	0.0	24.01±0.09	13.30±0.04	2013.09±1.11	4.685±0.013	0.2184±0.0003	1955.85±1.82
		10.0	23.17±0.04	12.57±0.02	1995.19±1.20	5.051±0.018	0.2061±0.0002	1965.05±1.46
		20.0	25.53±0.07	13.98±0.05	1784.61±1.05	5.517±0.011	0.1825±0.0003	2099.95±2.22
		30.0	27.86±0.06	15.31±0.03	1692.68±1.03	6.125±0.016	0.1664±0.0006	2190.75±1.64
		40.0	33.09±0.08	18.22±0.04	1613.89±1.12	6.731±0.011	0.1558±0.0004	2286.01±1.21
Uncertainty		1.8 %	1.6 %	1.9 %	2.1 %	3.0 %	1.5 %	
Sample code	WCC	3.672±0.003	9.260±0.018	2.271±0.002	0.872±0.002	1.818±0.001	3.984±0.001	
		3.664±0.003	7.945±0.016	2.450±0.002	0.881±0.001	2.184±0.001	4.029±0.002	
		3.493±0.003	6.854±0.012	2.639±0.002	0.933±0.002	1.793±0.002	3.892±0.003	
		3.460±0.001	6.033±0.012	2.813±0.002	1.022±0.002	1.751±0.002	3.526±0.002	
		3.451±0.003	5.343±0.010	2.989±0.003	1.170±0.002	1.735±0.002	2.989±0.003	
	YCC	3.937±0.002	5.547±0.010	2.934±0.002	2.010±0.001	1.579±0.001	2.861±0.002	
		3.920±0.002	5.256±0.005	3.013±0.001	2.038±0.002	1.998±0.002	2.895±0.002	
		3.748±0.001	4.869±0.010	3.132±0.003	2.189±0.002	1.564±0.002	2.782±0.001	
		3.708±0.002	4.488±0.017	3.262±0.005	2.444±0.001	1.526±0.003	2.496±0.002	
		3.689±0.001	4.222±0.011	3.362±0.004	2.895±0.003	1.520±0.003	2.173±0.003	
Uncertainty		2.4 %	3.8 %	3.8 %	2.0 %	1.0 %	1.0 %	

WCC:white clay composite; YCC:yellow clay composite

that the clay soils and HCWPAN utilised in this work have acceptable flow characteristics for manufacturing purposes. In terms of plasticity, the white clay has a greater index than the yellow clay.

The results in Table 3 show that after silica (SiO_2), the second most common chemical compound in each of the clay soils is alumina (Al_2O_3). Other main oxides in them include Fe_2O_3 and CaO . While CaO manages the structure and rupture threshold, the Al_2O_3 component contributes to increased mechanical resistance of a soil material. The lowest proportion of SiO_2 (with the highest fraction of Al_2O_3) may be responsible for higher plasticity and lower loss on ignition exhibited by the white clay. Though in the reverse, the same reason holds as regards the yellow clay. In each case, the contents of SiO_2 and Al_2O_3 fall within 50 % to 60 % and 10 % to 20 % respectively. According to the fact that clay used in bricks factories contains percentages of SiO_2 ranging between 50 % and 60 % [45], the clay soils utilised in this work can be regarded as potential raw materials for bricks making in factories. In the case of the HCWPAN, the proportion of CaO (56.78 %) exceeds those of other major oxides like SiO_2 (28.02 %), Al_2O_3 (1.62 %), and MgO (1.29 %). The combination of SiO_2 , Al_2O_3 , and Fe_2O_3 proportions in it yields 30.6 %. This value is less than 70 % which is the minimum requirement for a material to be pozzolanic [46], thus signifying that the HCWPAN is not a pozzolan. Due to application of hydrothermal calcination in this work, the proportion of CaO in the HCWPAN is greater by 11.6 % than the value (50.88 %) reported in the case of WPA [22] but very close to 58.24 % reported for the Portland limestone cement [47], thus reflecting an improvement in hydraulicity of the HCWPAN over the WPA.

In Table 4, it can be seen that the WCC samples record lower values of porosity and water absorption than the YCC samples. This may be attributed to variations in particle sizes of the clay soils used in this study (as earlier noted) since smaller particles agglomerate more easily than larger ones according to findings reported by Habadillah *et al.* [48]. At 10 % HCWPAN content, the lowest values of porosity and water absorption are obtained irrespective of the clay soil used. Actually, the difference in porosity values is about 8.48 % whereas the mean water absorption values differ by 4.57 %. This shows that, at such level of replacement, the CaO , Al_2O_3 , and SiO_2 present in the HCWPAN react optimally to enhance micro-aggregation and inter-particle packing. Consequently, the inter-particle voids are reduced, thereby decreasing the porosity and water uptake of the clay-based composite samples. However, incorporation of more than 10 % of the HCWPAN into each clay matrix brings about increase in porosity and water absorption of the resulting samples. For the WCC samples, the mean porosity values increase by 0.54 %, 4.63 %, and 10.01 % while the YCC samples exhibit increment by 1.52 %, 3.85 %, and 9.08 % at 20 %, 30 %, and 40 % levels of HCWPAN respectively, with respect to their blank sample. This, probably, is due to the nature of the HCWPAN which aligns with the submission of Zhang [49] that porous nano particles can influence soil properties very dramatically, even when they are present as a very small fraction. In addition to being the most porous and also exhibiting the highest degree of hydrophilicity compared to the clay soils, the HCWPAN contains numerous pores as a result of the tininess of its particles (≤ 80 nm). Therefore, the excess proportion of it in the composite mixes exercises a significant influence on the fabricated samples and promotes increment

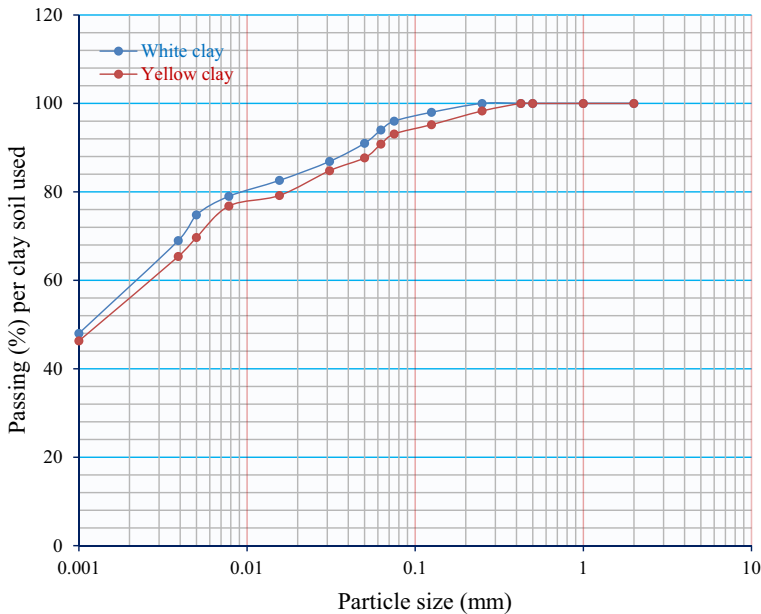


Fig. 2 Particle size distribution of the clay soil materials

in porosity and water uptake. In terms of improvement of durability, the results reveal that the use of HCWPAN at 10 % replacement level could yield clay-based composites with the lowest porosity and least tendency for water intrusion thereby enhancing their durability in service as building materials.

Since all the test samples developed and tested in this work were compacted under same laboratory conditions, a greater bulk density obtained for the reference white clay sample compared to its yellow counterpart may be due to dissimilarities in the particle sizes of the clay soils. The consequence of such non-uniformity in the particle sizes of the clay soils is that, in the same fixed volume, the pores (interstices) in the YCC samples are more than those present in the WCC samples. With incorporation of the HCWPAN at 10 %, 20 %, 30 %, and 40 % levels in the samples, respective mean bulk density values obtained are $31.20 \text{ kg}\cdot\text{m}^{-3}$, $323.86 \text{ kg}\cdot\text{m}^{-3}$, $451.85 \text{ kg}\cdot\text{m}^{-3}$, and $557.94 \text{ kg}\cdot\text{m}^{-3}$ less in the case of WCC samples but $17.90 \text{ kg}\cdot\text{m}^{-3}$, $228.48 \text{ kg}\cdot\text{m}^{-3}$, $320.41 \text{ kg}\cdot\text{m}^{-3}$, and $399.20 \text{ kg}\cdot\text{m}^{-3}$ less for the YCC samples than their reference value. The observed decreasing tendency is possible because the HCWPAN is the lightest among the materials used for development of the composite samples. In porous building materials, knowledge of liquid infiltration is also very vital for assessment of appearance and durability of such materials. Just like in the case of bulk density, the sorptivity of the reference samples is influenced by the pore size. In both cases, sorptivity increases with increase in the HCWPAN proportion and the WCC samples have greater values of it than their counterparts made with the yellow clay. This substantiates the assertion that the YCC samples contain pores of larger size and it also resonates with the observations of other

researchers like Ghazy [50] and Hallett [51] that a dry soil with larger pores has a lower sorptivity than a dry soil with smaller pores. The mean sorptivity values obtained by inclusion of the HCWPAN at 0 %, 10 %, 20 %, 30 %, and 40 % levels in the clay matrices produce a difference of 4.463, 4.450, 4.477, 4.604, and 4.761 (all in $10^{-4} \text{ m}\cdot\text{s}^{-1/2}$), respectively, between the WCC samples and YCC samples. Figure 3 depicts that bulk density and sorptivity of the studied samples are opposite in trends with respect to the percentages of the HCWPAN applied. Also, in the cases of bulk density, a sharp fall is observed between 10 % and 20 % loadings of the HCWPAN. On the contrary, sorptivity increases steadily with added proportions of the HCWPAN, a phenomenon that can be attributed to the ability of the HCWPAN to significantly penetrate the clay matrix and consequently create network to promote links which then enhance sucking up of water.

Porous building materials usually get subjected to the action of varying ambient conditions during the course of service. Thermal properties of soils influence how heat is partitioned within them. As a prominent component of dry soils, air greatly influences thermal conductivity of a soil whereas soil colour is a passive property that is solely determined by the mineral content(s) of the soil. The WCC sample containing 0 % of the HCWPAN is about 55.68 % more thermally conductive than its YCC counterpart. The implication of this tendency is that, if the blank samples are subjected to thermal influence under same conditions, a higher resistance to transmission of thermal energy will be offered by the YCC sample. This is possible because the yellow clay matrix contains a larger volume of interstices occupied by air, and as air is a very good thermal insulator, heat conduction is restricted more in the sample compared to the control sample made using the white clay. The approximate results obtained by utilising the HCWPAN at 10 % and 20 % levels with the yellow clay and white clay, respectively, are the same ($0.21 \text{ W}\cdot\text{m}^{-1}\cdot\text{K}^{-1}$). Observably, the highest or lowest marginal reduction ($0.0517 \text{ W}\cdot\text{m}^{-1}\cdot\text{K}^{-1}$ or $0.0106 \text{ W}\cdot\text{m}^{-1}\cdot\text{K}^{-1}$ respectively) in the mean thermal conductivity values is possible when incorporating the HCWPAN at 20 % into the white clay matrix or 40 % into the yellow clay matrix as the case may be. Apart from falling within $0.023 \text{ W}\cdot\text{m}^{-1}\cdot\text{K}^{-1}$ to $2.900 \text{ W}\cdot\text{m}^{-1}\cdot\text{K}^{-1}$ being the range of values recommended for heat-insulating and construction materials [52], all the values of thermal conductivity obtained in this work are less than the value reported for fired clay brick ($1.0 \text{ W}\cdot\text{m}^{-1}\cdot\text{K}^{-1}$) [53]. Due to variations in the pore sizes, the volume of air present in the pores may also be responsible for the specific heat capacity value of the blank YCC sample being greater than that of the reference WCC sample. The plots in Fig. 4 show that, with increasing proportions of the HCWPAN, thermal conductivity of the samples decreases whereas their specific heat capacity increases. From such phenomena, it can be inferred that the HCWPAN has lower thermal conductivity but greater specific heat capacity than either of the reference samples under consideration.

The volumetric heat capacity values of WCC samples are lower than those obtained for their YCC counterparts basically because the latter have lower values of bulk density. As the loadings of the HCWPAN increase, volumetric heat capacity of the resulting samples decreases. For up to 40 % increase in the HCWPAN content, the volumetric heat capacity values decrease by about 6.02 % in the case of utilising the white clay as matrix and 6.30 % for making use of the yellow clay material

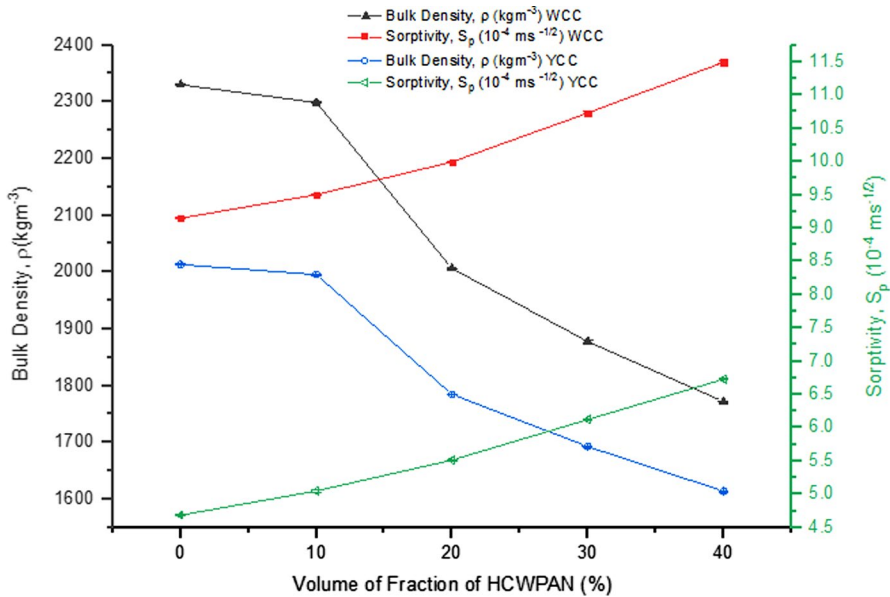


Fig. 3 Variations of bulk density and sorptivity of the samples with HCWPAN content

to develop the samples. Generally, the results mean that for a given volume, the YCC samples have greater internal energy storage ability than the WCC samples. Regarding thermal diffusivity, the values obtained in this study are lower for the YCC samples than in the cases involving the WCC samples. This implies that under same thermal front, the rate at which heat spreads to propagate temperature from one point to another is higher in the case of WCC samples compared to the YCC samples containing similar fractions of the HCWPAN. Though the inverse relationship between thermal diffusivity and volumetric heat capacity may account for this observation, lower values of thermal conductivity obtained for the YCC samples play a significant role. Irrespective of the clay soil material utilised as the matrix, the values of thermal diffusivity decrease with increasing contents of the HCWPAN.

Assuming any of the test samples is used as a walling material in a building, it is likely that it will be exposed to solar radiation in a 24-h cycle. In the event of such photothermal heating, periodic heat flow is bound to take place alongside the release of heat absorbed from the environment by the wall into the interiors of the building. The inverse relationship observed between thermal lag and thermal diffusivity of the studied samples is consistent with the expectation that, as the rate of spread of absorbed heat increases within a sample, a shorter time is required for the heat to be conducted through it. Low thermal conductivity and high specific heat capacity appear to be the two outstanding thermal factors that give rise to high thermal lag. Between the WCC and YCC samples, the two mean values of thermal lag that are very close are 2.989 h and 3.013 h, obtained by incorporation of the HCWPAN at 40 % and 10 % levels into the white clay and yellow clay materials respectively. Fgaier *et al.* [54] reported a thermal lag of 2.51 h for an unfired clay of thickness

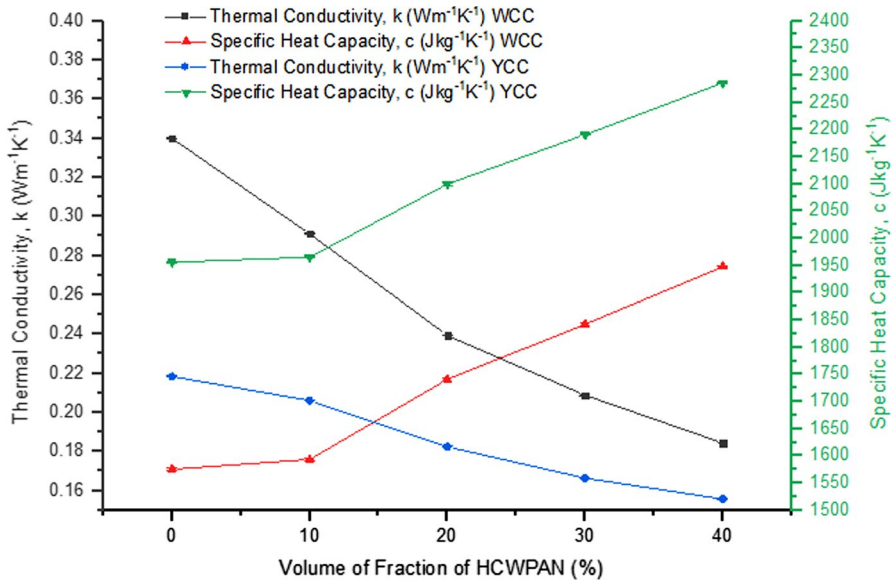


Fig. 4 Variations of thermal conductivity and specific heat capacity of the samples with HCWPAN content

104 mm and thermal conductivity $0.9 \text{ W}\cdot\text{m}^{-1}\cdot\text{K}^{-1}$. For the reference WCC and YCC samples (thickness being 30 mm each) tested in this work, the results show thermal lag of 2.271 h and 2.934 h respectively. It is obvious that if their thickness only is increased, the thermal lag would increase as well.

The degree of cohesiveness has a great deal of influence on the bonding strength of a material and it can be portrayed using some indices out of which one is static angle of repose. According to findings by Lumay *et al.* [55], a material's angle of repose increases as its cohesion increases. In that case, there is no doubt that in as much as cohesivity is high, bonding strength is also high thus leading to an increase in the mechanical strength of a material. Therefore, how strong or weak particles are held together in a material is determined by the strength of the existing bond and that in turn, has significant effect on flaking concentration of the material. The YCC samples are found to be flakier than the WCC samples, thus underlining the fact that cohesivity is higher in the white clay material compared to the yellow clay material used in this study. By extension, it implies that with similar proportions of the HCWPAN in them, the YCC samples are more susceptible to mechanical wear than the WCC samples. For the same reason, the WCC samples exhibit a higher strength to withstand bending load compared to the YCC samples. With reference to the blank sample, the clay-based composites fabricated from the white clay and yellow clay materials possess maximum flexural strength with increment of $(20.13 \pm 0.03) \%$ and $(26.54 \pm 0.07) \%$ respectively. Graphically, Fig. 5 illustrates that as the added proportion of the HCWPAN increases, the flaking concentration of the resulting clay-based composites increases. Such a remarkable possibility stems from the non-cohesive nature of

the HCWPAN due to a weaker bond in it compared to the bonding strength in either of the clay soil materials. The highest flexural strength value is observed at 10 % HCWPAN content, irrespective of the clay soil material used as the matrix in the composites formulation. Then after, a sharp decrease occurs as the HCWPAN content increases in the resulting composite samples. Plausibly, this may be that the silica content in the HCWPAN reacts optimally only when not more than 10 % level of it is utilized in the composite formulations. Beyond this proportion, the flexural strength of the resulting samples is mainly affected by the nature of the HCWPAN. Just like in the case of flexural strength, the highest compressive strength is obtained at 10 % HCWPAN content for each type of clay matrix used in this study. This simply reflects enhancement of particles bonding with aggregates as well as reduction of void spaces. CaO plays an important role in developing the compressive strength of a material. Thus, the possibility of the observed tendency may be attributed to the fact that at the introduction of water during samples fabrication, the CaO content of the HCWPAN reacts with the SiO_2 and Al_2O_3 found in each clay matrix to produce silicates of calcium. However, subsequent increase in the proportions of the HCWPAN introduces excess of it which may not have the opportunity to be utilised optimally in the matrix. As such, more pores and void fractions are formed and also, the inter-particle bonding that could have been formed by the particles of the soil is weakened as well. The resultant effect of this phenomenon therefore leads to the observed reduction in the compressive strength of the clay-based composites. With exception of YCC sample that contains at least 30 % of the HCWPAN, all other developed samples meet the minimum compressive strength requirement of 2.5 MPa stipulated in [56] for use as non-load bearing walling materials.

Comparatively, all the water absorption values obtained for the studied samples are less than those reported [17] for bricks made with fly ash and fired at 700 °C or 1050 °C. Improvement in compressive strength is possible with the HCWPAN especially at 10 % loading level, though nano silica yields up to 56 % increase in it [19]. At 0.05 level of significance, one-way analysis of variance yields calculated F-values of 9.95, 8.46, 2.99, 65.94, 4.81, 14.06, 12.06, 9.02, 11.57, 59.81, 3.12, and 19.19 between the mean values obtained for the WCC samples and YCC samples in the cases of porosity, water absorption, bulk density, sorptivity, thermal conductivity, specific heat capacity, volumetric heat capacity, thermal diffusivity, thermal lag, flaking concentration, flexural strength and compressive strength respectively. Against the critical value of 5.32, it simply means that significant difference does not exist in the results obtained for the samples' bulk density, thermal conductivity, and flexural strength only.

4 Conclusion

Based on the results of the experimental investigations conducted in this work, the following conclusions have been drawn:

The white and yellow clay soils utilised in this study contained fine sand, silt, and clay-sized particles but at varying proportions and that remarkably influenced the inter-particle packing as well as physical characteristics of the samples fabricated from them. When

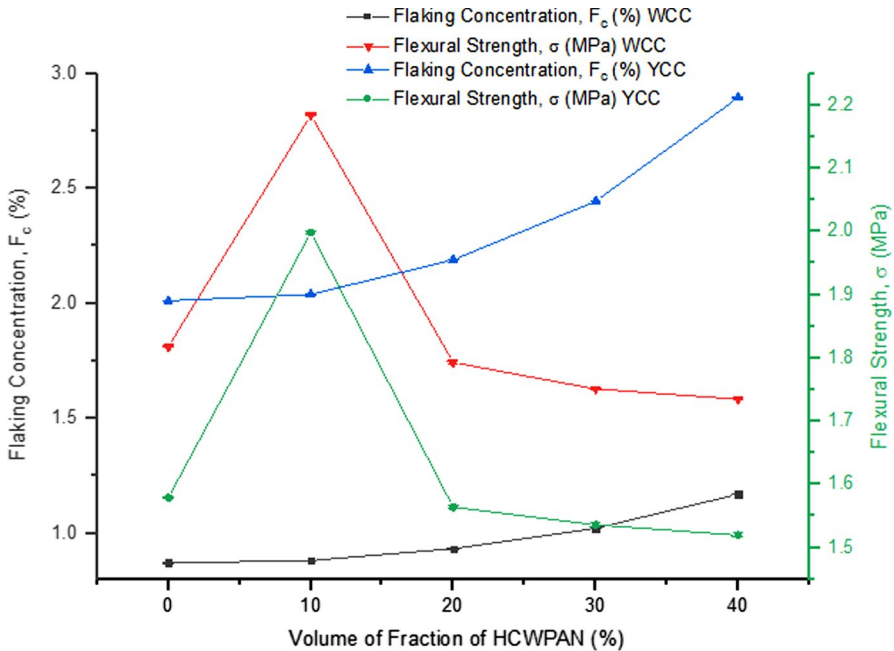


Fig. 5 Variations of flaking concentration and flexural strength of the samples with HCWPAN content

incorporating 10 % volumetric proportions of the HCWPAN into either clay matrix, the resulting clay-based composites possessed maximum flexural strength with increment of (20.13 ± 0.03) % and (26.54 ± 0.07) % as well as compressive strength with increment of (1.13 ± 0.05) % and (1.19 ± 0.09) % respectively. Increase in the content of HCWPAN enhanced improvement in the thermal insulation tendency of the developed composites over the control/blank samples. Samples developed with yellow clay exhibited greater tendencies for thermal insulation efficiency compared to those fabricated with white clay material. Clay-based composites made with 20 % and 40 % proportions of the HCWPAN in yellow clay and white clay materials respectively, compared very well in terms of their apparent porosity (25.53 % and 25.39 %) and water absorption (13.98 % and 14.15 %). For application as walling materials in passively cooled building design, samples fabricated with the HCWPAN were found to be capable of bettering thermal comfort than fired clay bricks as building materials especially in tropical regions. The results of this study clearly indicated that the clay soils can be chemically modified using varying volume fractions of the HCWPAN to develop clay bricks with satisfactory performances in buildings. Thus, tailoring waste papers for production of clay-based composites as described in this paper can serve as a safe way of managing the wastes and also improving the economy in building sector to ensure that housing is both affordable and safe. A future research could be designed to examine dependence of the clay bricks properties on calcination temperature and duration of HCWPAN.

Declarations

Conflict of interest The authors of the manuscript titled “Thermophysical and mechanical properties of clay-based composites developed with hydrothermally calcined waste paper ash nanomaterial for building purposes” declare that they have no known conflict of interest that could have appeared to influence the work reported herein.

References

1. B. Cox, J. Forshaw, *The Quantum Universe: Everything that can Happen Does Happen* (Da Capo Press, Allen Lane, 2011)
2. J. Chepkemoi, The top pulp and paper producing countries in the world, World Facts, Last updated: September 25, 2017, www.worldatlas.com
3. M. O'mara, How much paper is used in one day? Record Nations, Last updated: January 3, 2020, www.recordnations.com
4. A.E. Adeniran, A. Nubi, A. Adelopo, *Waste Manag.* **67**, 3–10 (2017). <https://doi.org/10.1016/j.wasman.2017.05.002>
5. R.O. Arazo, *Int. J. Res. Eng. Technol.* **4**, 263–267 (2015)
6. S. Kumar, H. Dhar, V.V. Nair, J.K. Bhattacharyya, A.N. Vaidya, A.B. Akolkar, *Env. Technol.* **37**, 2627–2637 (2016). <https://doi.org/10.1080/09593330.2016.1158322>
7. R.W.J. McKinney, *Technology of Paper Recycling* (Blackie-Academic and Professional. Chapman and Hall, New York, 1995)
8. R.M. Field, *World Acad. Art Sci.* **1**, 121–130 (1961). <https://doi.org/10.1007/978-94-017-6010-2>
9. J.A. Denton, *Society and the Official World: A Reintroduction to Sociology* (Dix Hills, New York, 1990)
10. M.S. El-Mahllawy, A.M. Kandeel, *HBRC J.* **10**, 82–91 (2014). <https://doi.org/10.1016/j.hbrj.2013.08.009>
11. L.M.A. Santos, J.A.S. Neto, A.F.N. Azerêdo, *Revis. Matêr.* **25**, 1–10 (2020). <https://doi.org/10.1590/51517-707620200001.0890>
12. S. Karaman, H. Gunal, S. Ersahin, *Constr. Build. Mater.* **20**, 348–354 (2006). <https://doi.org/10.1016/j.conbuildmat.2004.11.003>
13. E. Tsega, A. Mosisa, F. Fuga, *Am. J. Civ. Eng.* **5**, 21–26 (2017). <https://doi.org/10.11648/j.ajce.20170501.14>
14. P.W. Ihuah, *Afr. J. Econ. Sust. Dev.* **4**, 218–233 (2015). <https://doi.org/10.1504/ajesd.2015.071907>
15. P. Kara, *Épít.-J. Sil. Bas. Comp. Mat.* **67**, 12–18 (2015). <https://doi.org/10.14382/epítőanyag-jsbcm.2015.3>
16. S.P. Dunuweera, R.M.G. Rajapakse, *Adv. Mater. Sci. Eng.* **1**, 1 (2018). <https://doi.org/10.1155/2018/4158682>
17. H. Binici, O. Aksogan, H. Temiz, H. Kaplan, A. Ulusoy, *Int. J. Mater. Res.* **101**, 887–893 (2010)
18. H. Binici, R. Gemci, O. Aksogan, H. Kaplan, *Inter. J. Mat. Res.* **101**(7), 894–899 (2010)
19. M. Ghazavi, M. Bolhasani, *Proceedings of the 6th International Congress on Environmental Geotechnics*, New Delhi, India, 8 – 10 November (2010) 1490–1495
20. P. Javadzadeh, *J. App. Eng. Sci.* **9**, 139–144 (2019). <https://doi.org/10.2478/jaes-2019-0019>
21. U.W. Robert, S.E. Etuk, O.E. Agbasi, S.A. Ekong, Z.T. Abdulrazzaq, A.U. Anonaba, *Int. J. Thermophy.* **42**, 1–18 (2021). <https://doi.org/10.1007/s10765-020-02780-y>
22. B.M. Kejela, *J. Constr. Build. Mater.* **4**, 8–13 (2020). <https://doi.org/10.11648/j.ajcbm.2020401.12>
23. U.W. Robert, S.E. Etuk, O.E. Agbasi, G.P. Umoren, S.S. Akpan, L.A. Nnanna, *Acta Poly.* **61**, 749–761 (2021). <https://doi.org/10.14311/AP.2021.61.0749>
24. H.M.B. Al-Hashemi, O.S.B. Al-Amoudi, *Powd. Technol.* **330**, 397–417 (2018). <https://doi.org/10.1016/j.powtec.2018.02.003>
25. ASTM D 7928, ASTM International, West Conshohocken, 2017. <https://doi.org/10.1520/D7928-17>
26. ASTM D 4318, ASTM International, West Conshohocken, 2017. <https://doi.org/10.1520/D4318-17>
27. M. Bediako, *E.O.* 2015, 1 – 5. <https://doi.org/10.1155/2015/349401>
28. A.I. Inegbenebor, A.O. Inegbenebor, R.C. Mordi, N. Kalada, A. Falomo, P. Sanyaolu, *Int. J. Appl. Sci. Bio.* **4**, 21–26 (2016). <https://doi.org/10.3126/ijasbt.v4i1.14214>

29. ASTM C20, ASTM International, West Conshohocken, 2015. <https://doi.org/10.1520/C20-15>
30. U.W. Robert, S.E. Etuk, O.E. Agbasi, Iraqi J. Sci. **60**, 1704–1710 (2019). <https://doi.org/10.24996/ij.s.2019.60.8.7>
31. S.E. Etuk, O.E. Agbasi, U.W. Robert, Int. J. Energy Water Resour. (2021). <https://doi.org/10.1007/s42108-021-00123-7>
32. U.W. Robert, S.E. Etuk, O.E. Agbasi, G.P. Umoren, N.J. Inyang, Environ. Technol. Innov. **24**, 101869 (2021). <https://doi.org/10.1016/j.eti.2021/101869>
33. J.R. Philip, Soil Sci. **84**, 257–264 (1957). <https://doi.org/10.1097/00010694-195709000-00010>
34. U.W. Robert, S.E. Etuk, U.A. Iboh, G.P. Umoren, O.E. Agbasi, Z.T. Abdulrazzaq, Épít.-J. Sil. Bas. Comp. Mater. **72**(2), 72–78 (2020). <https://doi.org/10.14382/epitöanyag-jsbcm.2020.12>
35. U.W. Robert, S.E. Etuk, O.E. Agbasi, U.S. Okorie, A. Lashin, J. King Saud Uni.– Eng. Sci., 2021. <https://doi.org/10.1016/j.jksues.2021.10.005>
36. ASTM C518, ASTM International, West Conshohocken, 2017. <https://doi.org/10.1520/C518-17>
37. U.W. Robert, S.E. Etuk, O.E. Agbasi, S.A. Ekong, E.U. Nathaniel, A.U. Anonaba, L.A. Nnana, Polymer (2021). <https://doi.org/10.1007/s41050-021-00034-w>
38. U.W. Robert, S.E. Etuk, O.E. Agbasi, U.S. Okorie, Z.T. Abdulrazzaq, A.U. Anonaba, O.T. Ojo, J. Mech. Behav. Mater. **30**, 144–155 (2021). <https://doi.org/10.1515/jmbm-2021-0015>
39. ASTM C67/67M, Standard Test Methods for Sampling and Testing Brick and Structural Clay Tile, ASTM International, West Conshohocken, 2021.
40. N.E. Ekpenyong, G.P. Umoren, I.E. Udo, O.J. Yawo, Bri. Eng. **2**, 1–5 (2022). <https://doi.org/10.36937/ben.2022.4547>
41. U.W. Robert, S.E. Etuk, O.E. Agbasi, S.A. Ekong, J. Build. Mater. Struct. **7**, 95–104 (2020). <https://doi.org/10.5281/zenodo.3993274>
42. H. Lu, X. Guo, Y. Liu, X. Gong, Kona Powd. Part I. **32**, 143–153 (2015). <https://doi.org/10.14356/kona.2015002>
43. X. Guiling, C. Xiaoping, L. Cai, X. Pan, Z. Changsui, J. Part. Sci. Tech. **35**, 322–329 (2016). <https://doi.org/10.1080/02726351.2016.1154910>
44. USP, Powder Flow. In: The United States Pharmacopeia 30-National Formulary 25 Convention, Rockville, 2007.
45. P.M. Velasco, M.P.M. Ortíz, M.A.M. Giró, L.M. Velasco, Constr. Build. Mater. **63**, 97–107 (2014). <https://doi.org/10.1016/j.conbuildmat.2014.03.045>
46. ASTM C618, ASTM International, West Conshohocken, 2019. <https://doi.org/10.1520/C618-19>
47. I. Mehdipour, A. Kumar, K.H. Khayat, Mater. Des. **127**, 54–66 (2017). <https://doi.org/10.1016/j.matdes.2017.04.061>
48. S.K. Habadillah, Z. Haruna, M.H.D. Othman, A.F. Ismail, P. Gani, J. Asian Cer. Soc. **4**, 164–177 (2016). <https://doi.org/10.1016/j.jascer.2016.02.002>
49. G. Zhang, Adv. Meas. Model. soil Behav., ASCE (2007). [https://doi.org/10.1061/40917\(236\)37](https://doi.org/10.1061/40917(236)37)
50. A.E. Ghazy, Egypt J. Soil Sci. **22**, 57–67 (1993)
51. P.D. Hallett, Soil Water Res. **3**, S21–S29 (2008). <https://doi.org/10.17221/1198-SWR>
52. E.R.E. Rajput, *Heat and Mass Transfer*, 6 Revised. (S. Chand & Company PVT ltd, Ram Nagar, 2015)
53. D.R. Lide, *CRC Handbook of Chemistry and Physics* (CRC Press, Boca Raton, 2005)
54. F.E. Fgaier, Z. Lafhaj, F. Brachelet, E. Antczak, C. Chapiseau, Case Stud. Constr. Mater. **3**, 102–111 (2015). <https://doi.org/10.1016/j.cscm.2015.09.001>
55. G. Lumay, F. Boschini, K. Traina, S. Bontempi, J.C. Remy, R. Cloots, N. Vande walle, Powder Technol. **224**, 19–27 (2012). <https://doi.org/10.1016/j.powtec.2012.02.015>
56. NIS 87, Nigerian Industrial Standard: <http://www.stone> and www.stove.calbricks/bricks.html

Publisher's Note Springer Nature remains neutral with regard to jurisdictional claims in published maps and institutional affiliations.

Authors and Affiliations

Ubong Williams Robert¹ · Sunday Edet Etuk² · Joseph Bassey Emah¹ · Okechukwu Ebuka Agbasi³  · Ubong Asuquo Iboh¹

¹ Department of Physics, Akwa Ibom State University, Ikot Akpaden, Mkpata Enin, Nigeria

² Department of Physics, University of Uyo, Uyo, Nigeria

³ Department of Physics, Michael Okpara University of Agriculture, Umudike, Nigeria